Appl Phys B (2009) 96: 745–748
DOI 10.1007/s00340-009-3637-2

Applied Physics B
Lasers and Optics

RAPID COMMUNICATION

High-speed mixture fraction imaging

R.L. Gordon · C. Heeger · A. Dreizler

Received: 28 April 2009 / Revised version: 16 June 2009 / Published online: 17 July 2009

Abstract Advances in high-speed laser and camera technology have made scientific kHz repetition rate combustion and flow laser diagnostics feasible. While quantitative flow-field results have been shown to be possible via PIV, measuring scalars relevant to combustion such as mixture fraction, temperature and species concentrations is still a significant challenge. Tracer-LIF has proven to be a useful tool for imaging of mixture fraction. This paper highlights recent success at extending this technique for use at 9.5 kHz acquisition rate. The measurements are taken near the exit of an isothermal round jet seeded with acetone. Results taken at both maximum possible signal and a practical configuration for reacting flows are contrasted. Data are fully quantified and corrected for not only absorption, optical uniformity and laser pulse variation, but also for individual CMOS pixel offset and sensitivity.

PACS 33.50.Dq · 42.62.Fi · 06.60.Jn · 47.27.wj · 47.80.Jk

1 Introduction

Mixture fraction (ξ) imaging has been a key focus of experimental combustion diagnostics for some time. Of particular interest are the effects of turbulence-chemistry interaction and history effects on transient combustion phenomena, for example turbulent non-premixed ignition from a localised spark, which is important in many applications such as high altitude relight of a gas turbine, or gasoline direct injection IC engines [10]. Understanding mixing and flow field conditions prior to ignition requires a resolution of the time history prior to the event to fully understand the causes of failed and successful ignition [1]. It has already been shown for some transient combustion events that conditions up to several milliseconds prior can be relevant to the controlling mechanisms [2].

Advances in all-solid-state diode-pumped laser- and CMOS-camera technology have made cinematographic kHz application of common laser diagnostic techniques such as Mie scattering, PIV and PLIF achievable [3, 6, 8, 9, 15]. The long-term goal of these techniques is to provide quasi-4D simultaneous data on the flow-field and scalar fields in reacting flows. Progress has been made towards gathering comprehensive quantitative data from these techniques [2, 7], but an ongoing challenge for high-speed diagnostics is the quantification of scalar imaging techniques.

Decades of advances in CCD camera technology have led to high end cameras that have uniform pixel response with almost negligible non-linearities. With current CMOS-based cameras, there is a different, non-linear response for each pixel. Using an image intensifier also affects the ability to quantify the final image, and introduces signal diffusion effects that lead to gradient blurring. At high repetition rates, the laser pulse energies and consequent signals are comparatively low, which limits the application of standard techniques in quantitative diagnostics, and can require the use of image intensification.

Tracer LIF is a procedure of seeding a fluid with a marker that does not affect the fluid properties but is susceptible to laser excitation and fluorescence, providing an accessible method for monitoring the location of the seeded fluid [4, 5, 13, 14]. Acetone (CH_3COCH_3) has been a key tracer molecule for PLIF imaging of gaseous flows for the last two decades. It has been used for quantitative mixture fraction

R.L. Gordon (✉) · C. Heeger · A. Dreizler
Center of Smart Interfaces, Institute of Reactive Flows and Diagnostics, Petersenstraße 32, 64287 Darmstadt, Germany
e-mail: r.gordon@eng.cam.ac.uk
Fax: +49-6151-166555

imaging, and has further to determine temperature or pressure in various industrial configurations [11]. The goal of this paper is to report recent successes in developing this method for use at high repetition rates.

2 Experimental setup

The flow examined in this experiment is a simple round jet exiting a nozzle into mildly co-flowing air. The jet flow was provided by a 9.25 mm inner diameter Morel nozzle adaption at the exit of the concentric burner [12]. The bulk velocity was 12.5 $\mathrm{m\,s^{-1}}$ providing a Reynolds number of 7000. The Morel nozzle provides a short region of relaminarised flow, with instabilities forming around 2 jet diameters (D) downstream of the exit plane. The jet exits into a co-flowing air stream of 1.6 $\mathrm{m\,s^{-1}}$ (Re = 2400). All flow rates were controlled with Bronkhorst flow metres.

Bursts of 200 8 ns (FWHM) laser pulses at 9500 Hz were provided by an EdgeWave CX16II-E 80W Nd:YVO_4 diode-pumped slab laser. These were frequency quadrupled with a single-pass external crystal to 266 nm. The pulse burst spans 21 ms, averaging 1.0 mJ per pulse, with peaks up to 1.5 mJ. Absolute pulse energy is monitored with a pyroelectric fast-response energy metre (Coherent J-25MT-10KHZ) at the end of the beam path, and relative pre-absorption energies are monitored with a photo-diode (Thorlabs DET210). The photo-diode was tested for sensitivity to beam shape variations and calibrated to the results from the energy metre with no acetone flow and with laminar acetone flows of known concentration.

Images presented here were acquired with a LaVision HSS5 CMOS camera, both with and without a high speed Intensified Relay Optics (IRO) intensifier. Imaging at 9.5 kHz gives an active area of 512 × 512 pixels. Tests have also been conducted with an HSS6 camera at 768 × 768 pixels. Two collection optics were tested, first an image intensifier coupling optics with working focal distance of 38 mm that is constructed from two back-to-back 50 mm $f\# = 1.4$ lenses (effective $f\# = 0.7$). This was used to test maximum possible collection efficiency. A 85 mm Nikkor $f\# = 1.4$ was tested as an example of a more practical optical configuration.

Saturated acetone vapour was seeded into the jet flow via a controllable bypass seeder. The acetone is maintained at a constant temperature of 25°C in a thermostat controlled warming bath. Instantaneous seeding gas temperature was monitored with a thermocouple in the exit flow from the seeder. Adjustments for variations in vapour pressure due to acetone temperature were made with temperature data recorded at the instant of the image sequence. Acetone seeding rates were confirmed and calibrated under temperature controlled conditions, and the full-flow volumetric seeding fraction was approximately 30%.

2.1 Data processing

Recording long pulse bursts with high speed laser diagnostics usually requires the use of CMOS chip-based cameras. Key limitations of this architecture for quantitative scalar imaging are the non-uniformity of the sensitivity and offset of each pixel, and that the pixel signal response deviates from linearity, which is a key assumption in quantifying the data. To use a CMOS camera for quantitative diagnostics requires extensive calibration with a uniform intensity variable light source such as an Ulbricht Sphere. This has been undertaken for this work, and full details of the correction will be detailed in a further communication. It was found that the non-linearities can be as much as 10 to 15% at high counts, so correcting for these effects on a pixel-by-pixel basis is essential to conducting quantitative diagnostics with this equipment.

Each image from the CMOS camera is first corrected for the pixel response. The image is then dewarped, has a background subtraction and a white image correction. A 3 × 3 Median filter has been applied to all images during processing. As these image sequences have a known region of unity mixture fraction the individual beam profile and fluorescence reference were taken directly from each image. The images are then processed with an absorption model for the Acetone content based on the Beer–Lambert Law and measured temperature, assuming no significant beam steering (i.e. each pixel row is treated as a single ray). Absorption cross-section was confirmed with energy absorption tests with known acetone seeding rates. The out-of-plane beam width was measured by rotating the final sheet forming optic by 90° and capturing several hundred images in a uniform acetone vapour region.

3 Results

The reference tests for this method were made with maximum possible signal strength. The Acetone seeding bypass was set to zero, which leads to a seeding rate by volume of approximately 30%. The coupling optics were used for maximum collecting efficiency, and no filters were used. Under these conditions, it was possible to conduct the imaging measurements without the IRO, and peak raw spatial signal to noise ratio (SNR) of 70 to 80. These image sequences are suitable for use as a benchmark for further experiments. Close to the nozzle exit ($z/D = 1$) the flow has relaminarised from the Morel nozzle and has not yet formed turbulent instabilities. This region provides a location of repeatable, temporally and spatially stable steep gradients between the seeded jet and the ambient air. This serves as a good region for comparison of image quality. The key points of comparison are the single-frame (a) raw and (b) processed

Table 1 Comparative results for laminar test series. Results in brackets are for the final image of the burst sequence. Temporal SNR is calculated from an average of 25 × 25 individual pixels at $z/D = 0.75$, over 200 images

	Signal to noise ratios				Width of gradient (mm)		
	Raw	Processed	Mean	Temporal	$\xi = 0.2$–0.8	$\xi = 0.1$–0.9	$\xi = 0.05$–0.95
(1) Optimal imaging	72.5 (30.0)	197.7 (124.7)	228.8	96.2	0.30	0.49	0.67
(2) 85 mm lens	23.2 (14.8)	51.9 (45.2)	67.1	58.0	0.37	0.60	0.76
(3) 85 mm and 10% seeding	13.0 (10.8)	26.4 (23.5)	44.1	27.9	0.39	0.60	0.82
(4) As (3) with IRO	39.0 (33.8)	55.5 (41.2)	160.5	51.3	0.53	0.80	2.48

SNRs in a $\xi = 1$ region at the peak energy in the beam profile, a region of height = 0.5 mm (25 pixels), (c) spatial SNR from a mean of 200 images, (d) the average temporal SNR of single processed pixels in this same 25 × 25 pixel window, and the width of the gradient, taken as (e) $\xi = 0.2$–0.8, (f) 0.1–0.9, and (g) 0.05–0.95, all of which are reported in Table 1. The three measures of gradient width are presented to compare blurring effects, especially of the IRO. Data for the single frame cases (a) and (b) are presented for both the 50th and final (200th) images in the sequence. The pulse energy reduces significantly during the pulse burst, so it is important to note the reduction this has on the signal quality.

For the application of this method to a practical combustion experiment, these base conditions are not suitable. The working distance of the coupling optics is in the order of 40 mm, the optics are not adjustable in f-stop or focal distance, the image distortion due to vignetting and changes in Modulation Transfer Function (MTF) is large, the seeding density would significantly affect the combustion properties of the fuel, and laser energy absorption can be as high as 25% over a 1 cm beam path. To examine the impact of operating at more realistic conditions, sequences were taken with a more practical lens (Nikkor 85 mm, $f\# = 1.4$), and seeding densities below 10%.

It can be seen from Table 1 that implementing both these conditions necessitates the use of the IRO.

Introducing the IRO has a significant effect on the gradient width. Two-stage image intensifiers can display gradient spreading in regions of high gradient, as both a local MTF effect and a non-local blurring. This is most noticeable on the low-signal side of the gradient, and can be seen in the profile comparison ($z/D = 0.75$) in Fig. 1. For case (4), the profile from $\xi = 0.1$ noticeably flattens, and extends the low mixture fraction region almost to the edge of the imaging window.

A sequence of four frames taken at $z = 3D$ (centre of image) with setup (4) are presented in Fig. 2. The large scale structures move slightly less than a millimeter per frame, giving an axial velocity estimate of 8.5 m s^{-1} for these structures in the shear layer.

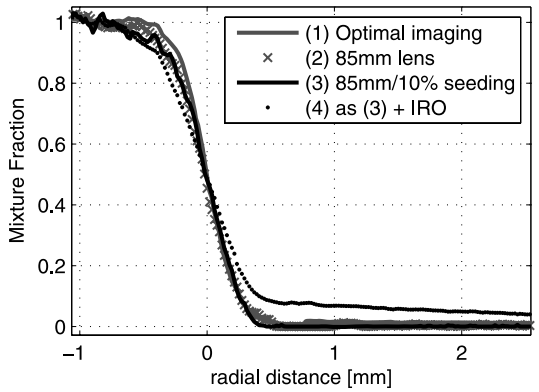

Fig. 1 Mixture fraction profiles at $z/D = 0.75$ for laminar flows. Symbols for (2) and line for (3) are almost co-linear

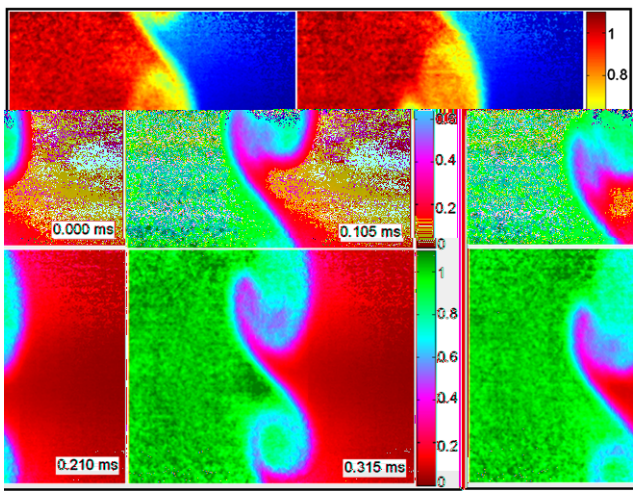

Fig. 2 Four consecutive images taken at $z = 3D$

3.1 Error assessment

The temporal and spatial RMS of the $\xi = 1$ regions provide useful information on the precision of the technique. Under best possible conditions, these are 1.0% and 0.4%, respectively. Under practical setup conditions with no intensifier these are 3.6% and 2.3% and with the IRO 1.9% and 0.6%. The impact of introducing the image intensifier is worth attention. Many practical combustion systems will have a sto-

ichiometric mixture fraction (the mixture fraction at which $\Phi = 1$) $\xi_{st} \leq 0.1$. In regions of steep gradients, the gradient blurring of the image intensifier can provide false readings from below $\xi = 0.2$, and as such render the experimental data untrustworthy for the mixture fractions of relevance. Best results would be obtained from an experiment where the IRO is not required, or one could minimise the error at the mixture fractions of interest by selecting a fuel-air mixture with a higher value for ξ_{st}.

Acknowledgements The authors gratefully acknowledge the sponsorship of the Deutsche Forschungsgesellschaft (GRK 1344, SFB 568 and EXC 259), and the contributions of V. Weber in implementing the CMOS correction algorithm.

References

1. S. Ahmed, E. Mastorakos, Spark ignition of lifted turbulent jet flames. Combust. Flame **146**, 215–231 (2006)
2. B. Böhm, C. Heeger, I. Boxx, W. Meier, A. Dreizler, Time-resolved conditional flow field statistics in extinguishing turbulent opposed jet flames using simultaneous highspeed PIV/OH-PLIF. Proc. Combust. Inst. **32**, 1647–1654 (2009)
3. I. Boxx, C. Heeger, R. Gordon, B. Böhm, M. Aigner, A. Dreizler, W. Meier, Simultaneous three-component PIV/OH-PLIF measurements of a turbulent lifted, C_3H_8-argon jet diffusion flame at 1.5 kHz repetition rate. Proc. Combust. Inst. **32**, 905–912 (2009)
4. N. Clemens, P. Paul, Effects of heat release on the near field flow structure of hydrogen jet diffusion flames. Combust. Flame **102**, 271–284 (1995)
5. O. Degardin, B. Renou, A. Boukhalfa, Simultaneous measurement of temperature and fuel mole fraction using acetone planar induced fluorescence and Rayleigh scattering in stratified flames. Exp. Fluids **40**, 452–463 (2006)
6. C. Fajardo, J. Smith, V. Sick, Sustained simultaneous high-speed imaging of scalar and velocity fields using a single laser. Appl. Phys. B, Lasers Opt. **85**, 25–30 (2006)
7. C. Heeger, B. Böhm, S. Ahmed, R. Gordon, I. Boxx, W. Meier, A. Dreizler, E. Mastorakos, Statistics of relative and absolute velocities of turbulent non-premixed edge flames following spark ignition. Proc. Combust. Inst. **32**, 2957–2964 (2009)
8. C. Kittler, A. Dreizler, Cinematographic imaging of hydroxyl radicals in turbulent flames by planar laser-induced fluorescence up to 5 kHz repetition rate. Appl. Phys. B **89**, 163–166 (2007)
9. M. Konle, F. Kiesewetter, T. Sattelmayer, Simultaneous high repetition rate PIV-LIF-measurements of CIVB driven flashback. Exp. Fluids **44**, 529–538 (2008)
10. E. Mastorakos, Ignition of turbulent non-premixed flames. Prog. Energy Combust. Sci. **35**, 57–97 (2009)
11. C. Schulz, V. Sick, Tracer-LIF diagnostics: quantitative measurement of fuel concentration, temperature and fuel/air ratio in practical combustion systems. Prog. Energy Combust. Sci. **31**, 75–121 (2005)
12. F. Seffrin, F. Fuest, D. Geyer, A. Dreizler, Lean stratified combustion: a generic premixed jet flame series for model validation, in *European Combustion Meeting*, Vienna University of Technology, Vienna, Austria (2009)
13. J. Smith, V. Sick, Crank-angle resolved imaging of biacetyl laser-induced fluorescence in an optical internal combustion engine. Appl. Phys. B, Lasers Opt. **81**, 579–584 (2005)
14. M. Thurber, R. Hanson, Simultaneous imaging of temperature and mole fraction using acetone planar laser-induced fluorescence. Exp. Fluids **30**, 93–101 (2001)
15. A. Upatnieks, J. Driscoll, S. Ceccio, Cinema particle imaging velocitmetry time history of the propagation velocity of the base of a lifted turbulent jet flame. Proc. Combust. Inst. **29**, 1897–1904 (2002)